ELSEVIER

Catalysis Today 39 (1998) 281–291

CATALYSIS TODAY

Experimental aspects of X-Ray absorption spectroscopy

George Meitzner*

Edge Analytical Inc., P.O. Box 2365, Stanford CA 94309, USA

Abstract

X-ray absorption spectroscopy (XAS), including X-ray absorption near-edge spectroscopy (XANES) and extended X-ray absorption fine-structure spectroscopy (EXAFS), provides physical and chemical information on almost any element regardless of matrix or conditions. Experimental factors that are critical to successful measurements, including general beamline configuration and energy resolution, in situ cell design, detector gases and common artifacts are discussed. This review is intended to assist during experimental setup and data collection. Published by Elsevier Science B.V.

1. Introduction

X-ray absorption spectroscopy (XAS) is a powerful technique that provides chemical information on a single element in a sample, as do NMR and Mössbauer Spectroscopies. It also provides direct physical structural information, like X-ray diffraction, but describes the environment of a single element in the sample. XAS has been reviewed often [1–3].

X-ray absorption edges were first observed by DeBroglie [4] in 1916. The associated fine structure was recorded in 1920 by Fricke [5] and the Fricke's paper provides a good benchmark against which progress in experimental methods can be judged. Fricke noted that problems presented by sample thickness, spectral resolution and detector sensitivity, required solutions specific to the short wavelength of the radiation. Ironically, he concluded incorrectly that the Ar spectrum he measured showed no fine structure due to problems with his setup. (This lack of fine structure in the Ar spectrum is now understood to be a consequence of the isolated atom structure of Ar gas). As reported by Fricke, his X-ray source was a Cooldige Tube. The dispersive element was either a sucrose or a rock-salt crystal and the detector was a photographic plate. The image was rendered into a graph by an optical densitometer constructed from an incandescent lamp, a clock motor, a thermocouple and a galvanometer. The Ti and S images and corresponding spectra are shown in Fig. 1. The Ar spectrum mentioned above was not published.

Important advances were reported by Van Nordstrand [6] in exploiting edges and by Sayers, Stern and Lytle [7] who demonstrated that the fine structure could be understood by Fourier Transformation. Beginning in the mid 1970s, spectra have mainly been measured at synchrotron sources, which provide continuous spectra [8] smoother and several orders of magnitude stronger than the conventional X-ray sources (Fig. 2).

2. Synchrotron beamline- the XAS spectrometer

A representative beamline, X-10C at National Synchrotron Light Source (NSLS), is shown in Fig. 3. The

*Corresponding author.

0920-5861/98/$32.00 Published by Elsevier Science B.V.
PII S0920-5861(97)00114-4

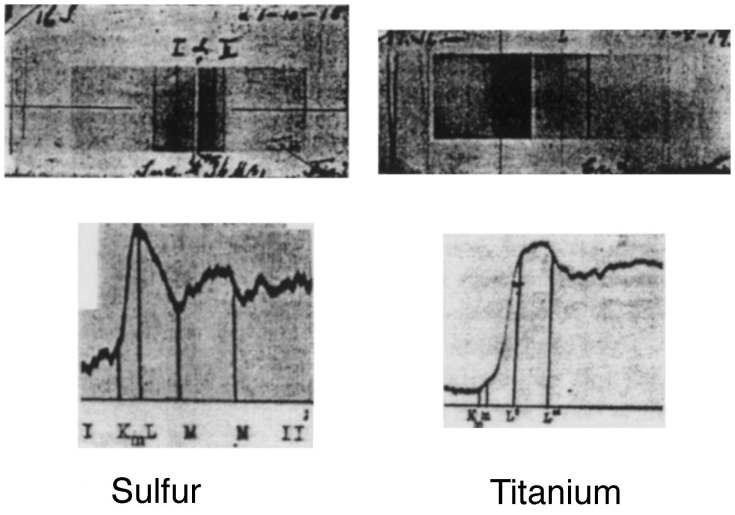

Fig. 1. X-ray absorption spectra in photographic emulsions on microscope slides (top) and on paper from [5]. No attempt has been made to align the images with the graphs. The samples were elemental sulfur and TiO_2. The dispersive element were a sugar crystal for the S spectrum and a rock salt crystal for the Ti spectrum.

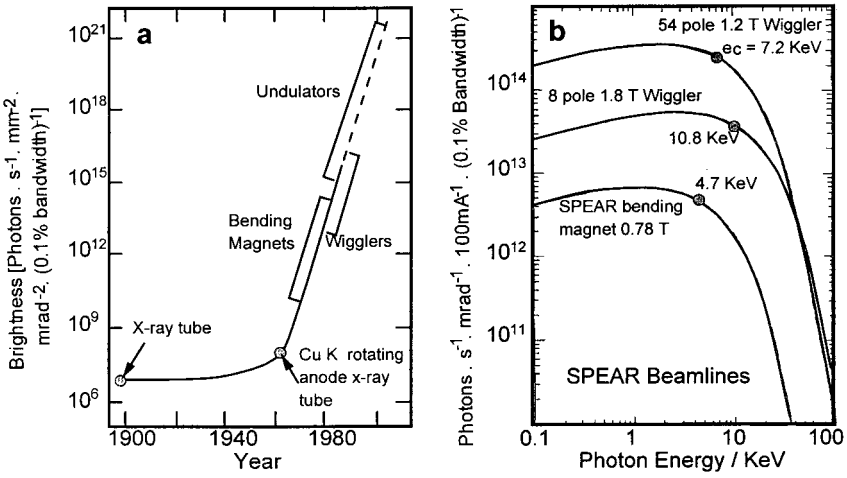

Fig. 2. (a) Evolution of brightness of X-ray sources [8]. Bending magnets, wigglers and undulators are all synchrotron sources. Undulators yield a sharp line spectrum and are not generally suitable for XAS. (b) Characteristic synchrotron spectra, with the SSRL source SPEAR operated at 3 GeV. The X-ray tube and rotating anode spectra are broad and continuous, punctuated by a few intense spikes. These spectra are well below the bottom of the graph.

optical components are the source, the slit assembly in front of the monochromator, the monochromator and the mirror. Some beamlines incorporate a mirror between the source and the monochromator, to improve collimation of the beam and thereby improve the best resolution achievable without sacrificing intensity. Not all beamlines include a mirror between the monochromator and the sample; but when present its function is to focus the beam and/or reject harmonics. Another slit assembly may be included at the end

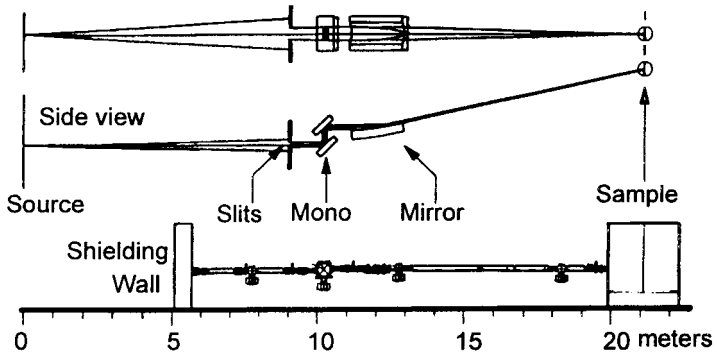

Fig. 3. National Synchrotron Light Source (NSLS) beamline X-10°C.

of the beamline to define and crop the beam. Whereas these components are found on many laboratory spectrometers, the X-ray beamline presents some unique experimental problems. First, the synchrotron source is not controllable by the experimenter, so data are taken when it is turned on, including at night and on holidays. Earlier problems with poor duty cycle (fraction of the usable time), frequent loss of ring current, beam motion and other types of source instability are largely under control. Also, the demand for synchrotron beam time continues to exceed the supply, although this problem is diminishing as new sources are built.

A second experimental problem probably unique to synchrotron beamlines, is that the X-ray beam is deflected through angles that may be very small and the corresponding lever-arms are long. For example, measuring a Mo K edge spectrum at 20 000 eV using Si (220) monochromator crystals implies angles of less than 10° between the X-ray beam and monochromator crystals. The angle of incidence of the X-ray beam on a mirror designed to reject harmonics may be in the order of 1°. Note in Fig. 3 that the beamline is 20 m long and the distance from the mirror to the sample is 10 m. Thus alignment of optics must be very precise, because small errors result in large errors in beam trajectory, recorded as noise as the beam moves over the face of an inhomogeneous sample.

A third experimental complexity, if not problem, is that most beam lines are unique, controlled by unique computer systems and software.

3. Data collection software

All the XAS data collection software programs with which we have experienced share key functions common to scanning spectrophotometers. These include commands to identify the inputs, or scalars, to be monitored and written; to define the spectrum to be collected in terms of starting and ending energies, spacings between points and integration times per point; to measure the 'offsets', or dark currents read from the detectors in the absence of X-rays; to begin a sweep; and for miscellaneous functions such as recalibrating the monochromator and moving it to a new energy. Fig. 4 illustrates a typical spectrum 'setup', which includes 3 differently defined data collection regions.

4. X-ray energy resolution

In general XAS places a rather low premium on energy resolution compared, for example, to X-ray diffraction. One reason for this, is that features in the extended fine-structure region of a spectrum are naturally broad compared to the most degraded resolution possible from a beamline with a distance of 10 m between a point source and the monochromator. Another reason is that many of the absorption edges of interest are at high energy, so that the natural broadening of the core-hole means the narrowest feature that can be observed is broader than the best resolution of which the beamline is capable. In most cases the principle reason for paying attention to

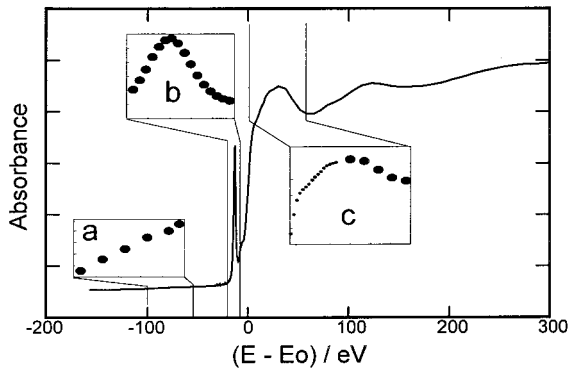

Fig. 4. Representative X-ray absorption spectrum (Cr in Na_2CrO_4) illustrating a typical spectrum setup. The pre-edge region (a) is structureless and widely spaced points (10 eV) serve only to define the slope. A fine interval between points (0.3 eV here) in the near-edge region (b) is necessary to define narrow features. The EXAFS region (c) extends 1000 eV or more beyond the edge. Less resolution is needed. Here the transition from the edge to the EXAFS region is shown.

beamline resolution, is to enable meaningful comparisons among spectra measured in different times and places.

Lifetime broadening is discussed by Krause, et al. [9] and data from the reference are shown in Fig. 5(a). Note that natural widths are not purely lifetime effects, since the K and L_{III} core-holes of the same energies have significantly different broadenings. However, broadenings do generally increase with energy. Assuming beamline resolution ΔE_{photon} is dominated by source divergence, then it is given mainly by the differentiation of Bragg's Law, defined in terms of energy in Eqs. (1a) and (1b)

$$\Delta E_{photon} = 2E_{photon}\cot\left[\sin^{-1}\left[\frac{hc\sqrt{h^2+k^2+l^2}}{4\pi a E_{photon}}\right]\right] \times \tan\frac{x/2}{y} \quad (1a)$$

$$\cong 2E_{photon}\cot\left[\sin^{-1}\left[\frac{12398.5}{2dE_{photon}}\right]\right]\tan\frac{x}{2y} \quad (1b)$$

where y is the distance from the source to the most restrictive aperture before the monochromator and x is the vertical size of the aperture. The constants h and c are Planck's Constant and the speed of light, respectively. (h, k and l) are the Miller Indices and a is the

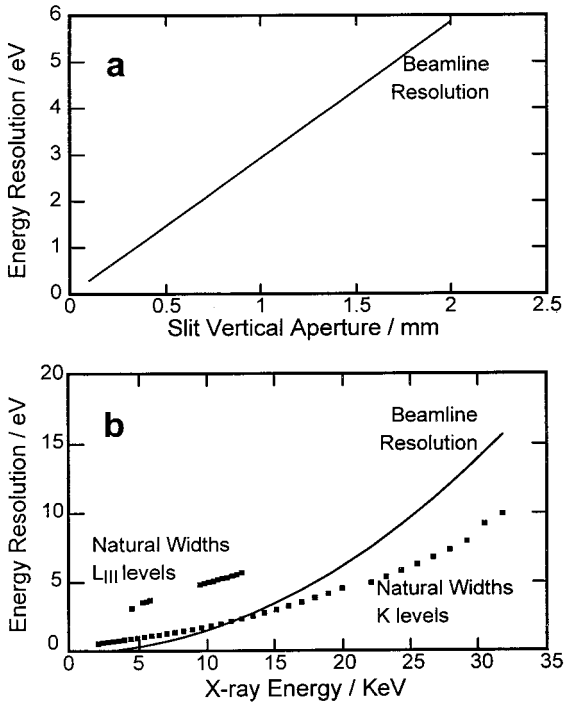

Fig. 5. (a) Dependence of beamline resolution on pre-monochromator slit vertical aperture (no collimating mirror). This calculation assumes X-ray energy of 10 000 eV; Si (220) crystals; slit 10 m from point source. (b) Solid line: Dependence of beamline resolution on X-ray energy; Si (220), slit vertical aperture 0.5 mm, 10 m from source. Discrete points: Natural widths of K and L_{III} levels from Krause [9].

cubic lattice constant of the monochromator crystals. In (Eq. (1b)), the interplanar spacing d has been substituted for $a/\sqrt{h^2+k^2+l^2}$ and the constant 12398.5 has units of eV·Å. E_{photon} is the actual energy at which the measurement is made [10,11]. Eqs. (1a) and (1b) does not describe the resolution of beamlines with a collimating mirror between the source and monochromator, with the objective of improving resolution without a corresponding loss of intensity. Other components of resolution are given by the horizontal aperture in front of the monochromator and the Darwin Width, a description of the perfection of the crystallinity of the specific crystals in service. Fig. 5(a) compares Eqs. (1a) and (1b) with natural widths, for Si (220) crystals and slit vertical aperture of 0.5 mm and Fig. 5(b) shows how resolution

ΔE_{photon} depends on slit vertical aperture x, with Si (220) crystals, at 10 KeV.

5. Sample preparation

Samples for X-ray absorption spectroscopy are solids, liquids, or gases. The lowest acceptable concentration of the absorbing element depends strongly on the matrix of other elements in the sample and the detectors being used, but a few hundred parts per million is probably always approachable. At high concentrations, above ≈2 wt.%, it is usually most appropriate to measure the transmitted intensity while at lower concentrations it may be better to measure the fluorescent intensity. A statistical basis for the choice is discussed in [2]. It is not too difficult to measure the electron yield from electrically conducting samples [12–15], which provides information on approximately the top 1000 Å of sample [16] and avoids the problem of thickness distortions to be discussed below. The most commonly used detectors are ion chambers because the brightness of synchrotron sources makes it necessary to accommodate high counting rates with a wide linear range. For very dilute samples, solid state cryogenic detectors are used because they offer high efficiency and are able to lower the background by rejecting all but the fluorescence photons associated with the core hole of interest.

Sample preparation for XAS should not be taken casually. A spectrum is not necessarily a good one just because it shows no noise; in general thickness distortions can be detected only by preparing serial dilutions or thickness series and inspecting the consequent spectra for differences in contrast. The true uniform thickness to give a desired absorbence can be calculated from:

$$M = \frac{A}{\sum_i f_i(\mu/\rho)_i}\left(\ln\frac{I_o}{I}\right) \quad (2)$$

where I_o and I are the incident and transmitted intensity, respectively; A is the area of the sample to be prepared and f_i and $(\mu/\rho)_i$ are the weight fractions and mass absorption coefficients of the elements i in the sample at the energy near an absorption edge [17]. The maximum value of $\Delta\ln(I_o/I)$ across the absorption edge should be kept below about 1.5 where the Δ refers to the change in absorbence across the edge. The mass absorption coefficients $(\mu/\rho)_i$ are defined by McMaster [18] in Eq. (3):

$$(\mu/\rho) = \left(\sum_{k=0}^{3} A_k(\ln E)^k\right)/C \quad (3)$$

Where E is the photon energy in K eV and A_k and C are coefficients that are tabulated by McMaster for each element. Eqs. (2) and (3), taken together, indicate that fractional transmission (I/I_o) depends in a complicated way on atomic number (choices of A_k and C), photon energy E and path length M/A. It has been my experience that attempts to estimate transmittance through a given material more precisely than 'probably transparent' or 'probably opaque', are futile.

Thin or dilute samples present problems in obtaining a sufficient signal or signal to noise ratio, but concentrated samples can also be a problem. In this context concentrated means the highest value of the product μx to be measured is greater than one. This is true, for example, if the thickness x of a film of a pure element is greater than the value of $1/\mu$ of the element where μ is the linear absorption coefficient. It is also true if the X-ray beam probes a sample to a depth that contains this thickness of the absorbing element.

There are a wide variety of mechanisms for distortion of spectra when the sample is thick and/or inhomogeneous. Fluorescence spectra are always distorted to some extent and a sample thin enough for fluorescence measurement is one for which the spectrum is judged as an acceptable approximation to the true spectrum. Fig. 6 shows how contrast is lost in a fluorescence spectrum from a homogeneous sample, as the sample thickness increases. Distortion is absent only for an infinitely thin sample.

Fig. 7 shows sulfur K-edge fluorescence spectra from aqueous solutions of sodium thiosulfate in a range of concentrations. Taken individually all the spectra appear reasonable, but the relative change in intensity of the second peak indicates that most if not all of the samples were too thick. Note that powders are poor samples for fluorescence, since the smallest particle size might be about 10 μm, often much too thick and it is very difficult to decrease particle size by grinding. The type of distortion associated with fluorescence measurements can be corrected (although not

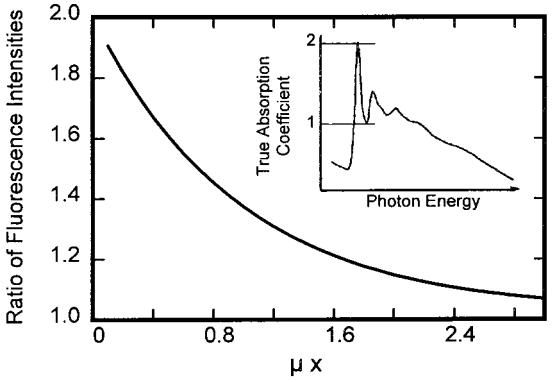

Fig. 6. Ratios of the measured fluorescence yields from a sample for which the true spectrum is shown in the inset, as a function of sample thickness. For the Cu K edge, a value $\Delta\mu x=1$ corresponds to a Cu film 5 μm thick, or to an areal loading of 45 mg cm^{-2}.

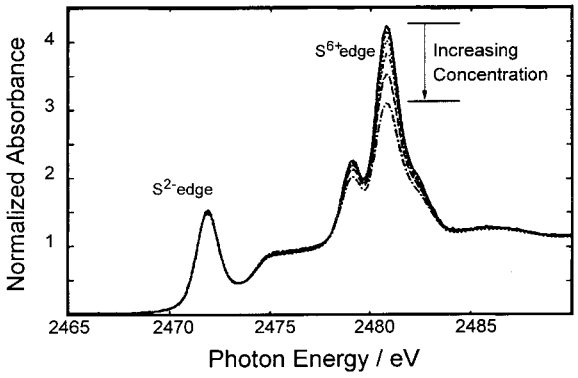

Fig. 7. Fluorescence yield sulfur K X-ray absorption edge spectra of aqueous thiosulfate, in a series of concentrations 25 mM through 1 mM. The feature at about 2472 eV was hardly affected, but the stronger features at 2480 eV were very sensitive to concentration, showing that most or all of the solutions were too concentrated or too thick.

perfectly) if the path length and sample composition are accurately known [19].

Transmittance spectra are distorted if the sample is either thick or inhomogeneous [20]. Thick samples encourage 'leakage' of X-rays that are not attenuated in a way that correctly reflects the true absorption coefficient, either because there will be thin areas in the sample, or because harmonics in the X-ray beam are not absorbed. Fig. 8 shows the decrease in amplitude of EXAFS that results, as a function of sample thickness and of percent of leakage. For this reason

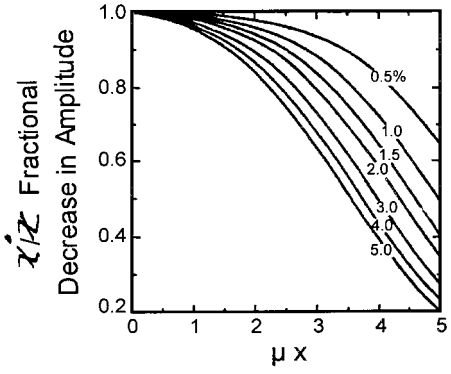

Fig. 8. EXAFS amplitude reduction as a function of $\Delta\mu x$ for various leakage levels. Leakage occurs because the sample has thin spots or pin holes, or because the harmonic in the beam is hardly attenuated by the sample.

samples prepared by collecting powders on tape or filter paper should be usually avoided.

There are other mechanisms by which thick samples lead to distorted spectra. McHugh [10] pointed out that thick samples may present a very large range of values of absorbence that taxes the linear range of the electronics. Pease [21] discussed the distortion that results from a finite monochromator bandpass, that gets worse as the energy bandpass broadens and perversely, as the sample gets thinner.

6. X-ray absorption cell

Methods for preparing samples that require no in situ treatments have been described in the literature [17,22,23]. A general approach has been to use an Al plate with a slot into which the sample is packed and retained by polymer films [24] on the front and back. As noted above, caution should be exercised with solid samples. Some are extremely difficult to prepare as suitable samples for transmittance or fluorescence and electron yield detection [12–15] should be considered.

Although the task seems simple of heating a sample in a controlled atmosphere, in a configuration that also allows an X-ray beam to pass thorough the sample but not the extraneous hardware, this problem has given rise to a wide range of designs. For samples that can be prepared under the controlled atmosphere and then transported, but must not be exposed to air, a cell

comprising a flow section that can be isolated by valves, with windows at one end, has been widely used [25]. Many other designs have been published for transmittance or combined fluorescence and transmittance measurements [26,27] including at high pressure [28–30] and from supercritical samples [31]. X-ray cells that make possible simultaneous X-ray absorption and diffraction measurements have also been described [32–34].

The following check list might be helpful for designing an in situ cell for a specific experiment:

1 What data are to be taken?
Transmittance, fluorescence, electron yield, X-ray diffraction...
2 What in situ conditions will be required?
Maximum temperature and pressure; corrosive conditions and tolerance of leaks.
3 What type of sample and experiment are intended?
Gas, liquid powder, wafer, supercritical sample...
Will temperature control or fluid flow characteristics be critical?
4 Will measurements be required below ≈7 KeV?
X-rays are weakly penetrating: path length within cell must be minimized, fluorescence detection will be required and highly transparent windows must be used.

A cell designed for fluorescence measurement should also accommodate transmittance, because anything behind a fluorescence sample will scatter or fluoresce and raise the background or interfere.

7. X-ray cell window materials

Properties of many prospective window materials, including polymers, are described in the Goodfellow catalog [35]. Fig. 9 shows transmittance through various window materials. Choices can be classed as polymers, metals and ceramics. The polymers are transparent, inexpensive and convenient. Available polymer films span an impressive range of properties. For example, polypropylene, in the 2.5 μm thickness, is very transparent but mechanically and thermally poor. On the other hand, polyimide (Kapton) in a 8 μm thickness is much more expensive, stronger and has an upper working temperature of 250–320°C. Metals suitable for windows include Be, Al and Ti. Be is

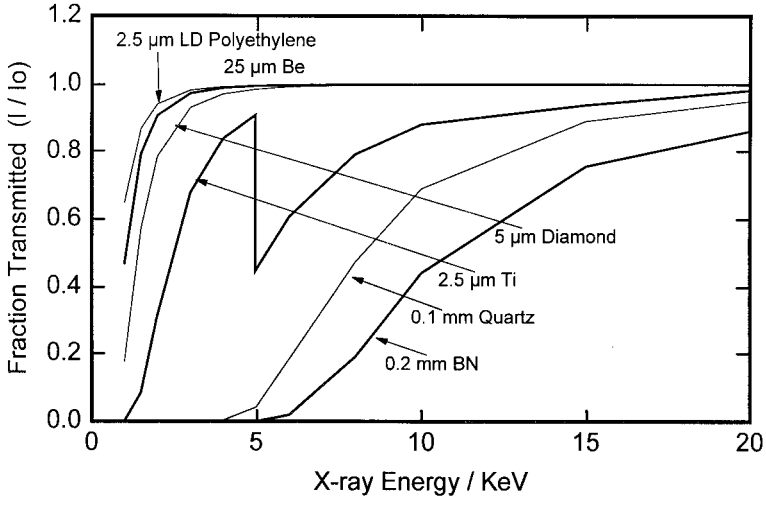

Fig. 9. Fraction of transmission vs. energy through various window materials [18]. The thicknesses shown are all commercially available. 25 μm Be is a vacuum tight grade. The Ti K edge falls at about 5 KeV. Fractional transmittances are hard to estimate because they are nonlinear in energy, path length and atomic number.

very transparent and chemically inert [28,36]. Al is reasonably transparent but not very strong and melts at 600°C. Ti was our own choice for a large fluorescence window exposed to corrosive environment, very high temperature and pressure up to ≈10 psi. Ceramics suitable for windows include BN and quartz (SiO_2). An elegant cell design by Clausen et al. [33] obtains excellent thermal and gas flow characteristics, while exploiting the high strength of a quartz capillary to hold the sample.

8. Ion chamber gases

Ion chambers are the most commonly used detectors for XAS, probably because they are linear through a very wide range of signal strength and are also inexpensive and durable. Sensitivity depends on the gas in the chamber. Fig. 10 shows transmittance by several commonly used ion chamber gases. In general a heavier gas is used to obtain sensitivity to higher energy X-rays. The appropriate gas absorbs enough to yield a sufficient signal, but the I_o detector, transmits sufficiently to satisfy the detectors that are beyond the sample. The last detector beyond the sample may absorb all the remaining beam for maximum sensitivity. A statistical analysis of how the choice of gases should be made is included in [2]. Note in Fig. 10 that Kr actually absorbs more strongly than the much more expensive Xe, i.e. confers greater sensitivity, in the energy range between about 20 and 34 KeV. Gas mixtures and low pressure gases can be used in principal to optimize detector performance; however leak-tight detectors are required and these are not widely available.

9. Common artifacts and problems with data

Glitches are defects in spectra that are typically differential in shape, only a few eV wide and perfectly reproducible. They result from Bragg diffraction in the monochromator, off crystal planes that are not parallel to the crystal surfaces, or more generally due to multiple diffraction conditions. The consequent sharp excursions in the beam intensity are recorded in spectra if they do not normalize out between the incident intensity I_o and the signal intensity. If the diffraction artifact affects only the harmonic wavelength, then it probably does not normalize out. Glitches are pronounced when the X-ray beam is cropped by a window in the X-ray cell, between the incident intensity monitor I_o and the transmittance detector I_1 [37]. In fact, all kinds of noise are exacerbated when the beam is thus cropped. This is probably the most common reason for poor data from appar-

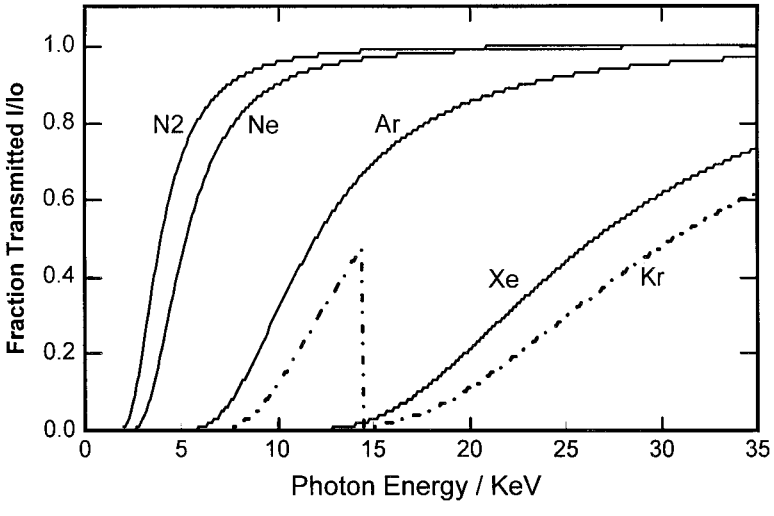

Fig. 10. Fraction of transmission vs. energy through common ion chamber detector gases. The path length was 10 cm. Notice that Kr is more strongly absorbing (more sensitive) than the more expensive Xe in the energy range from 15 to 35 KeV.

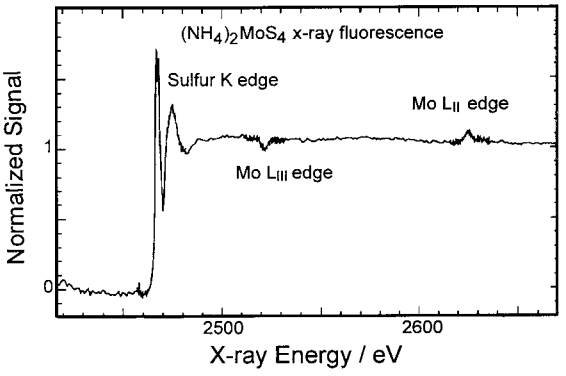

Fig. 11. Total fluorescence yield spectrum from the sulfur K edge in $(NH_4)_2MoS_4$. Two Mo L edges fall within the spectrum. The Mo L_{III} edge is inverted because it absorbs incident X-rays and casts a shadow on the S, but the S absorbs the Mo fluorescence line. The Mo L_{II} edge is weaker and shades the S less and the S is less strongly absorbing at the position of the corresponding fluorescence line. Fluorescence yield spectra are subject to an array of such artifacts.

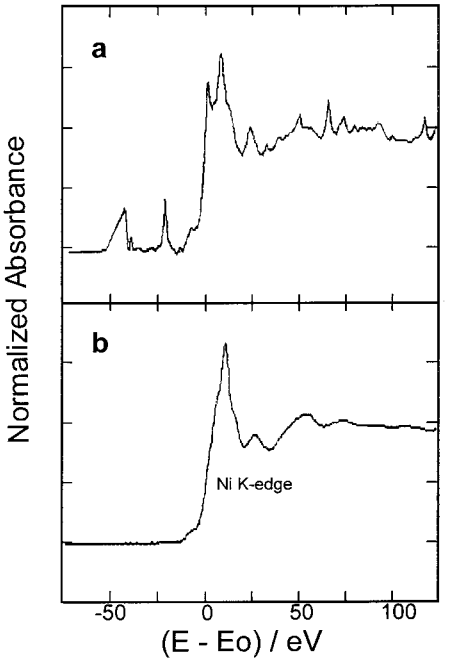

Fig. 12. (a) Fluorescence yield spectrum from Ni supported on α-Al_2O_3. The spikes result from diffraction by Al_2O_3 into the fluorescence detector. (b) The cell was made to vibrate by attaching an engraving tool, in order to time-average the diffraction paths.

ently concentrated samples. To avoid these problems, the beam should be trimmed in front of the first detector, to a size that can pass through all orifices without clipping.

Distortion of spectra resulting from excessive sample thickness has already been discussed. However, loss of amplitude is only the most common consequence. A variety of puzzling artifacts can result from excessively thick samples. Fig. 11 shows a sulfur K-edge spectrum from $(NH_4)_2MoS_4$, measured by fluorescence. The Mo L_{III} edge at 2520 eV is inverted because it shadows the S and decreases the intensity of S K_α fluorescence, but the corresponding Mo L_η fluorescence is strongly absorbed by the sulfur. Conversely, the Mo L_{II} absorption edge is right-side up; it is weaker than the L_{III}, but the corresponding Mo L_γ fluorescence line is absorbed much less by the sulfur.

Crystalline samples can cause problems for fluorescence data collection, by diffracting into the fluorescence detector. For powders or polycrystalline solids, this artifact looks like intense low frequency noise (Fig. 12(a)), but is reproducible as long as the sample is not moved. Also, the transmittance spectrum is relatively clean, if it can be measured. This problem can be controlled with an energy discriminating detector (Ge solid-state cryogenic type) by accepting only the fluorescence but rejecting scatter. Another approach that works regardless of the detector type, is to spin the sample, but this is not practical for the in situ measurements. We have controlled the problem during in situ measurements (Fig. 12(b)) by making the cell vibrate.

Other common problems are associated with gas flow through the cell and ion chamber detectors. The tubing from the gas source, through the ion chambers and out to the vent forms a large chamber with a low resonance frequency. Detector gas can begin surging in this chamber, causing pressure oscillation in the detectors and oscillation in the data that might look like EXAFS (Fig. 13). Also, the cell and ion chambers purge slowly. If a spectrum is measured while they are purging, then a kink typically appears in the spectrum at a point where the scan rate changes between the pre-edge and near-edge region.

10. Data analysis

Although this review is concerned with data collection, the experiment is not complete until spectra that

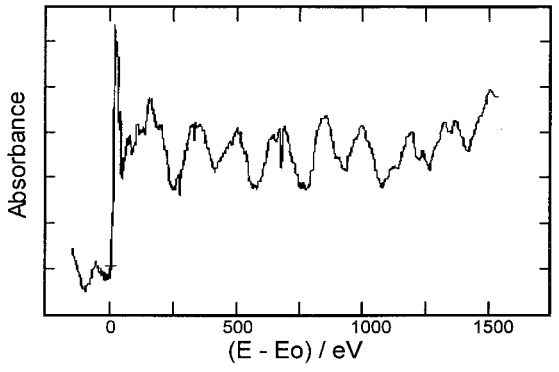

Fig. 13. A severe example of the damage to a spectrum that results when the detector gas surges in the chamber formed by the tubing and detectors. The more typical low amplitude oscillation looks like EXAFS, but notice that it extends into the pre-edge region and that it is periodic in time (not in K space).

are usable have been measured and this cannot be established without some data analysis. Several excellent data analysis packages are now generally available. These include FEFF [38], XCURVE [39], XDAP [40] and XAFSPAK [41].

On-the-fly data analysis concerns include finding the edge position of standard samples to evaluate the calibration of the monochromator. Two such markers should be measured to verify the monochromator tracking, i.e. that 1000 eV on the energy scale reflects 1000 eV of true sweep. Glitches are sometimes used as energy markers. Also, a reference spectrum should serve to evaluate resolution. For this purpose the pre-edge feature at the metallic copper K-edge is useful. With respect to sample preparation and performance of electronics, contrast between weakly and strongly absorbing features should be checked. Other artifacts discussed above leave their signature in spectra; the most treacherous are extraneous oscillatory signals that look like EXAFS. These can usually be recognized because they have excessive amplitude, or because they are periodic in time or energy (monochromator position) but not in K-space.

11. Conclusion

XAS would be an astoundingly difficult experiment if it were approached as are most other spectroscopic measurements. The XAS source alone is extremely complex. Ideally, the specialized teams who operate and maintain the source and beamline are transparent and the spectroscopist need worry only about the physics and chemistry of the sample. I have found this is often approached closely at SSRL. Still, Figs. 7, 11–13 are intended in part to convey that there are many ways for a spectrum to go wrong. Be cautions and seek simple non-chemical explanations when the data are really surprising.

Acknowledgements

The author wishes to thank Dr. Britt Hedmann and Dr. Graham George of the Stanford Synchrotron Radiation Laboratory (SSRL), Fremont, CA, for graciously allowing the use of Fig. 7 and Fig. 11 respectively and for innumerable helpful discussions. Some work described herein was done at SSRL which is operated by the Department of Energy, Office of Basic Energy Sciences. Research was also carried out in part at the National Synchrotron Light Source, Brookhaven National Laboratory, which is supported by the U.S. Department of Energy, Division of Materials Sciences and Division of Chemical Sciences.

References

[1] H. Bertagnolli, T.S. Ertl, Angew. Chem. Int. Ed. Engl. 33 (1994) 45.
[2] P.A. Lee, P.H. Citrin, P. Eisenberger, B.M. Kincaid, Rev. Mod. Phys. 53 (1981) 769.
[3] M.J. Fay, A. Proctor, D.P. Hoffmann, D.M. Hercules, Anal. Chem. 60 (1988) 1225A.
[4] M. DeBroglie, J. Phys. 5 (1916) 161.
[5] H. Fricke, Phys. Rev. 16 (1920) 202.
[6] R.A. Van Nordstrand, Advances in Catalysis, 12, 19 (1960); A. Meisel (ed.), Proc. Int. Symp. Radiation and Chemical Binding, 23 and 24 September 1965, Karl Marx Universität, Leipzig, Germany, 1966, p. 255.
[7] D.E. Sayers, E.A. Stern, F.W. Lytle, Phys. Rev. Lett. 27 (1971) 1204.
[8] H. Winick, Scientific American 257 (1987) 88.
[9] M.O. Krause, J.H. Oliver, J. Phys. Chem. Ref. Data 8 (1979) 329.
[10] B.J. McHugh, Ph.D. Thesis, Yale University, 1991.
[11] T. Matsushita, H-O. Hashizume, in E-E. Koch, (Ed.), Handbook on Synchrotron Radiation, North-Holland Publishing Co., New York, Vol. 1A, 1983. pp. 261–314.

[12] N.J. Schevchik, D.A. Fishcer, Rev. Sci. Instrum., 50, (1979) 577; G.G. Long, D.A. Fischer, D.J. Krugyer, G.A. Danko, D K. Tanaka, Phys. Rev. B 39 (1989) 10651.
[13] M.E. Kordesch, R.W. Hoffman, Phys. Rev. B 29 (1984) 491.
[14] T.K. Sham, R.G. Carr, J. Chem. Phys. 83 (1985) 5914.
[15] F.W. Lytle, R.B. Greegor, G.H. Via, J.M. Brown, G. Meitzner, J. de Phys. 47 (1986) C8–149.
[16] Z.W. Bonchev, A. Jordanov, A. Minkova, Nucl. Instru. Meth. 70 (1969) 36.
[17] E.D. Eanes, J.L. Costa, A. MacKenzie, W.K. Warburton, Rev. Sci. Instrum. 51 (1980) 1579.
[18] W.H. McMaster, N. Kerr Del Grande, J.H. Mallett, J.H. Hubbell, Compilation of X-ray Cross Sections, UCRL-50174 Sec. II Rev. 1, Technical Information Center, United States Department of Energy, 1987.
[19] L. Tröger, D. Arvaitis, K. Baberschke, H. Michaelis, U. Grimm, E. Zschech, Phys. Rev. B 46 (1992) 3283.
[20] E.A. Stern, K. Kim, Phys. Rev. B 23 (1981) 3781.
[21] D.M. Pease, Appl. Spectroscopy. 30 (1976) 405.
[22] J. Wong, Nucl. Inst. Meth. Phys. Res. 238A (1985) 554.
[23] M.A. Marcus, W. Flood, Rev. Sci. Instrum. 62 (1991) 839.
[24] M.J. Solazzi, American Laboratory, November 1985, p. 124.
[25] B.S. Clausen, B. Lengeler, R. Candia, J. Als-Nielsen, H. Topsøe, Bull. Soc. Chim. Belg. 90 (1981) 249.
[26] F.W. Lytle, P.S.P. Wei, R.B. Greegor, G.H. Via, J.H. Sinfelt, J. Chem. Phys. 70 (1979) 48499.
[27] F.W.H. Kampers, T.M.J. Maas, J. VanGrondelle, P. Brinkgreve, D.C. Koningsberger, Rev. Sci. Instrum. 60 (1989) 2635.
[28] R.A. Dalla Betta, M. Boudart, K. Foger, D.G. Loffler, J. Sanchez-Arrieta, Rev. Sci. Instrum., 55 (1984) 1210; By SEM inspection, Be windows were unaffected by exposure to air or 12 MPa 2% H_2S/H_2 after 8 h, with H_2S/H_2 temperature 690 K and maximum measured window temperature 320 K.
[29] T.L. Neils, J.M. Burlitch, J. Catal. 118 (1989) 79.
[30] D.R. Allan, R. Miletch, R.J. Angel, Rev. Sci. Instrum. 67 (1996) 840.
[31] D.M. Pfund, J.G. Darab, J.L. Fulton, J. Phys. Chem. 98 (1994) 13102.
[32] M.G. Samant, G. Bergeret, G. Meitzner, M. Boudart, J. Phys. Chem. 92 (1988) 3542.
[33] B.S. Clausen, G. Steffensen, B. Fabius, J. Villadsen, R. Feidenhans'l, H Topsøe, J. Catal. 132 (1991) 524.
[34] A.J. Dent, M. Oversluizen, G.N. Greaves, M.A. Roberts, G. Sankar, C.R.A. Catlow, J.M. Thomas, Physica B 208 (1995) 253.
[35] Goodfellow Corporation, Berwyn, PA.
[36] Goodfellow reports that Be resists attack by air or water to red heat. Brush-Wellman, Fremont, CA, which specializes in Be windows, makes no mention of corrosive attack on Be in their literature or Materials Safety Data Sheet for Be.
[37] E.A. Stern, K-Q. Lu, Nucl. Inst. Meth. 195 (1982) 415.
[38] FEFF Project, University of Washington, Seattle, WA.
[39] Synchrotron Radiation Source, Lancashire, UK.
[40] XAFS Services International, Utrecht, The Netherlands.
[41] G. George, Stanford Synchrotron Radiation Laboratory, Stanford, CA.